Journal Pre-proof

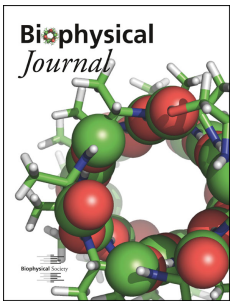

Modulation of structural heterogeneity controls phytochrome photoswitching

Emil Gustavsson, Linnéa Isaksson, Cecilia Persson, Maxim Mayzel, Ulrika Brath, Lidija Vrhovac, Janne A. Ihalainen, B. Göran Karlsson, Vladislav Orekhov, Sebastian Westenhoff

PII: S0006-3495(19)30948-8

DOI: https://doi.org/10.1016/j.bpj.2019.11.025

Reference: BPJ 9968

To appear in: *Biophysical Journal*

Received Date: 9 October 2019

Accepted Date: 20 November 2019

Please cite this article as: Gustavsson E, Isaksson L, Persson C, Mayzel M, Brath U, Vrhovac L, Ihalainen JA, Karlsson BG, Orekhov V, Westenhoff S, Modulation of structural heterogeneity controls phytochrome photoswitching, *Biophysical Journal* (2019), doi: https://doi.org/10.1016/j.bpj.2019.11.025.

Modulation of structural heterogeneity controls phytochrome photoswitching

Emil Gustavsson,[1]* Linnéa Isaksson,[1]* Cecilia Persson,[2] Maxim Mayzel,[2] Ulrika Brath,[2] Lidija Vrhovac,[1] Janne A. Ihalainen,[3] B. Göran Karlsson,[1,2] Vladislav Orekhov,[1,2] Sebastian Westenhoff[1†]

* These authors contributed equally to this work
† To whom correspondence should be addressed: westenho@chem.gu.se

1. Department of Chemistry and Molecular Biology, University of Gothenburg, Gothenburg, Sweden
2. Swedish NMR center, University of Gothenburg, Gothenburg, Sweden
3. Department of Biological and Environmental Science, University of Jyväskylä, Jyväskylä, Finland

Running title: Structural heterogeneity in phytochromes

Significance

Phytochromes are light-sensing proteins found in plants, fungi and bacteria. They are very primitive equivalents to human eyes and essential for the organism to change their growth or development in response to environmental light conditions. Limited experimental information about the dynamics and signaling mechanism for phytochromes exist. In this study, we investigate the structural dynamics using solution NMR spectroscopy. The pioneering experiments reveal that a specific element important for signaling, called the “PHY tongue”, transforms from a structurally heterogenous dark state, with two or more conformations present, to an ordered and homogenous light state. We suggest that upon illumination, this transition locks the phytochrome in the activated state and that this explains how phytochromes modulate their photoactivity.

Abstract

Phytochromes sense red/far-red light and control many biological processes in plants, fungi, and bacteria. Although crystal structures of dark and light adapted states have been determined, the molecular mechanisms underlying photoactivation remains elusive. Here we demonstrate that the conserved tongue region of the PHY domain of a 57kDa photosensory module of *Deinococcus radiodurans* phytochrome, changes from a structurally heterogeneous dark state to an ordered light activated state. The results were obtained in solution by utilizing a laser-triggered activation approach detected on the atomic level with high-resolution protein NMR spectroscopy. The data suggest that photosignaling of phytochromes relies on careful modulation of structural heterogeneity of the PHY tongue.

Keywords: Phytochrome, molecular dynamics, NMR, protein structure, phototransduction

Introduction

Phytochromes are light-sensing proteins which monitor the level, intensity, duration and color of environmental light (1–3). They control numerous light-dependent processes in plants, fungi and bacteria (4–8). Phytochromes are promising targets in the expanding field of optogenetics to allow precise light control of various internal cellular processes (9). Absorption of red light by the dark-adapted (Pr) state leads to formation of the light activated (Pfr) state. The dark state can be recovered by far-red light.

Most phytochromes are homodimeric proteins with the common conserved domain architecture PAS-GAF-PHY (Per/Arndt/Sim-cGMP phosphodiesterase/adenyl cyclase/Fh1A-phytochrome specific) as the photosensory core module (10, 11). A covalently linked bilin chromophore is attached via a thioether linkage to a conserved cysteine in either the PAS domain (bacteria) or GAF domain (cyanobacteria and plants) (12). In cyanobacteria and bacteria, the output domain often consists of a C-terminal histidine kinase, but in plants and fungi a so-called N-terminal extension and C-terminal output domains, consisting of two PAS domains and a kinase-like domain, are present.

Phytochromes with a PAS-GAF-PHY photosensory module have a characteristic hairpin loop, called ”the tongue” (residue 444-476), which extends from the PHY domain to the chromophore binding pocket in the GAF domain (Fig. 2). Crystallographic analysis has indicated that this tongue changes between two distinct structures from β-sheet configuration in dark to α-helical in light state (13–15). This refold has been connected to opening of the dimer in-crystallo and in solution, which most likely result in modification of the output domain. The tongue has therefore a key role in signal transduction (13).

The above-mentioned structural models were built under the assumption that the protein is a static entity with well-defined states in dark and light. However, proteins are not static entities in living organisms, rather their structures are highly dynamic. This is of functional relevance (16).

Nuclear Magnetic Resonance (NMR) spectroscopy is a powerful tool for examining the structure and dynamics of biological macromolecules, but NMR analysis of large proteins, like bacteriophytochromes, are difficult due to increased spectral complexity and sensitivity losses (17). These obstacles are probably the reason for why solution-state NMR has only been applied to phytochrome PAS

or PAS-GAF domains and not the complete photosensory core (18–22). The chromophore binding pocket has previously been studied using both solution and solid-state NMR. With solid-state NMR, two hydrogen bond and charge distribution configurations have been detected in the chromophore binding pocket of a cyanobacterial phytochrome in the dark-adapted state (23). Recent solution NMR of a chromophore binding fragment of a red/green cyanobacteriochrome has confirmed this in agreement with optical spectroscopy (18, 24). Resonance Raman and time-resolved infrared spectroscopy have detected two chromophore conformations in light state in cyanobacterial and plant phytochromes (25).

The evolutionary conserved tongue region (residue 444-476) is in close contact with the chromophore, and the prevailing hypothesis is that upon illumination, distinct conformational changes in the chromophore binding pocket are transduced to the tongue region resulting in refolding (13, 26–28). However, limited experimental information about the dynamic contribution of the tongue region of phytochromes exist. In this study, we aim to investigate the correlation of dynamics and photoactivation with focus on the important tongue region in phytochromes. To do this, we used high-resolution protein solution NMR spectroscopy of the complete PAS-GAF-PHY photosensory module combined with a laser-triggered approach to control the photochemical state of the phytochrome.

Materials and Methods

The construct for the *Deinococcus radiodurans* monomeric phytochrome PAS-GAF-PHY fragment has previously been cloned (pET21b) and transformed into BL21(DE3) cells (29). The K177A, K476A and K460A mutant constructs were made with the Quikchange Lightning Site-Directed Mutagenesis Kit (Agilent Technologies; Stevens Creek Blvd, Santa Clara, CA). The clones were verified by sequencing and transformed into competent BL21(DE3) cells.

Small-scale overnight cultures of the phytochrome were prepared in Luria-Bertani (LB) media. 4 ml of the cultures were inoculated to 200 ml of M9 media (Na_2HPO_4, KH_2PO_4, NaCl, NH_4Cl, d-glucose, thiamine, $MgSO_4$, $CaCl_2$, H_2O). 0.02 g of all unlabeled amino acids, except for lysine, were solubilized with M9 media and added to the cultures. Methionine and cysteine were solubilized with DTT and M9

media. To tryptophane and tyrosine, HCl and KOH were added respectively until the amino acids were completely solubilized. The cultures were grown at 37°C at 180 rpm. 15 minutes before induction, 0.2 g of all unlabeled amino acids, except for lysine, were added again together with 20 mg of ^{13}C,^{15}N-labeled lysine. At OD 0.64, the temperature was decreased to 22°C and 1mM IPTG was added. Induction continued for 24 hours before the cells were harvested. An Emulsiflex C3 (Avestin; 2450 Don Reid Dr, Ottawa, ON, Canada) was used to disrupt the cells followed by a 30 minutes centrifugation at 10 000 rpm. 3 mg of biliverdin (BV) hydrochloride (Frontier Scientific; 195 South 700 West, Logan, UT) was dissolved in 1 ml 30 mM Tris buffer pH 8.0 with 8M NaOH titrated until BV was completely solubilized. The cell lysates and the BV were incubated dark overnight at 4°C. The samples were filtered and loaded onto a 5 ml HisTrap HP column (GE Healthcare; 500 West Monroe Street, Chicago, IL). The proteins were eluted with a linear gradient of imidazole with 30 mM Tris, 50 mM NaCl, 300 mM imidazole pH 8.0. The proteins were concentrated with 30 kDa MWCO Vivaspin (Sartorius; Otto-Brenner-Strasse 20, Göttingen) to 3 ml and loaded to a HiLoad 16/600 Superdex 200 pg column (GE Healthcare; 500 West Monroe Street, Chicago, IL) equilibrated with 30 mM Tris pH 8.0. Eluted fractions were concentrated as described above. Buffer was exchanged by centrifugation to 25 mM NaPi, 50 mM NaCl pH 6.9. UV-Vis was used to verify that the proteins could photoswitch, and the purity was checked using SimplyBlue Coomassie (Invitrogen; 168 Third Avenue, Waltham, MA) staining of Mini-PROTEAN TGX Stain-Free gel (Biorad; 1000 Alfred Nobel Drive, Hercules, CA). PageRuler Prestained Protein Ladder (Fermentas; BWI Commerce Park 7520 Connelley Dr. Suite A, Hanover, Maryland) was used as a standard.

Cells were adapted to D_2O by streaking out on M9-agar plates containing increasing concentration of D_2O (25%, 50%, 75%, 100%). Colonies from the 100% D_2O plate were picked and 5 ml overnight cultures of the phytochrome were prepared in M9 media (Na_2HPO_4, KH_2PO_4, NaCl, $^{15}NH_4Cl$, u-^{13}C-d-glucose, thiamine, $MgSO_4$, $CaCl_2$, D_2O). 1 ml of one of these cultures was inoculated to 50 ml of M9 media. This culture was further used to inoculate 2x500 ml of M9 media. At OD 0.6, the temperature was decreased to 30°C and 1 mM IPTG was added. Induction continued for 22 hours before the cells were harvested. Sample was purified according to the protocol stated above.

0.8 mM of $^{13}C,^{15}N$-lysine-labeled phytochrome samples (wt, K476A and K460A) were mixed with 10% D_2O, 1x Complete EDTA-free (Roche; Grenzacherstrasse 124, CH-4070, Basel) and 0.02% azide. 3 mm shigemi tubes were used. To measure the phytochromes in the dark-adapted state, the samples in the NMR tube were illuminated in darkness using a 780 nm LED (1.5mW) for 10 minutes. The samples were injected into the magnet in darkness. To convert the samples to the light state, a 660 nm LED (14.5mW) was used for illumination for 10 minutes.

0.8 mM of $^{2}H,^{13}C,^{15}N$-labeled phytochrome sample was mixed with 10% D_2O, 1x Complete EDTA-free (Roche; Grenzacherstrasse 124, CH-4070, Basel) and 0.02% azide. A 3 mm shigemi tube was used. To measure the phytochrome in the dark-adapted state, the sample in the NMR tube was illuminated in darkness using a 780 nm LED for 10 minutes. The sample was injected into the magnet in darkness. To convert the sample to the light state, a 660 nm LED-laser (400mW) was connected to an optical fiber with a diffuser tip (Laser components; Werner-von-Siemens-Str. 15, 82140 Olching) which was inserted into the sample inside the 3 mm shigemi tube (30). The sample was illuminated for 5 seconds every 20 minutes during data acquisition to continuously keep the sample in the light state.

NMR experiments were performed at 15°C, 25°C, 45°C and 55°C on Bruker spectrometers with Larmor frequencies of 800 MHz and 700 MHz equipped with 3mm triple resonance TCI cryoProbes. [$^{1}H,^{15}N$]-TROSYs were recorded for both the dark-adapted and light state for the wt, K460A mutant and the K476A mutant. Visualization and verification of the assignment were performed using the CCPN software package (31).

NMR experiments were performed at 45°C on a Bruker spectrometer with a Larmor frequency of 800 MHz equipped with a 3mm triple resonance TCI cryoProbe. The automated backbone assignment was obtained using a previously reported assignment platform (32), which uses non-uniformly sampled 3D TROSY type experiments (HNCO, HNCA, HN(CO)CA, HNCACB, HN(CO)CACB, HN(CA)CO) combined with Targeted acquisition (TA) and statistical validation. The details of this TA platform will not be discussed further in this paper. [$^{1}H,^{15}N$]-TROSYs were recorded before and after all 3D spectra, and also between each TA cycle to verify that the sample was identical throughout the entire measurement

time. 3D [^{15}N]- NOESY-TROSYs were also recorded for both states and used during the manual assignment process. Verification of the automatically assigned residues and manual assignment were performed using the CCPN software package (31).

The secondary chemical shifts $\Delta\,\delta = \delta - \delta_{rc}$ were obtained by subtracting the random coil value for each residue (δ_{rc}) from the chemical shift for the same residue (δ). The random coil data was obtained from Wishart and Sykes (33). The web server chemical shift index (CSI 3.0) was used to identify the location of secondary structure and random coil in the dark-adapted and light state of the phytochrome.

UV-Vis spectra were recorded at 45°C with the scanning wavelengths of 280-850 nm. The sample was illuminated with a 780 nm LED for 10 minutes and the spectrum was measured directly after (0h). After a 72h incubation in the dark, the UV-Vis spectrum was measured again.

Results

Backbone chemical shift assignment of the dark and light state

We report solution-state NMR data of the monomeric (509 residues) photosensory module (PAS-GAF-PHY) fragment of the *Dr*BphP. The experiments were performed as described in materials and methods.

[^{1}H^{15}N]-TROSY spectra (Fig. 1) and a set of non-uniformly sampled 3D TROSY-type H-N-C spectra were recorded for both states. This set formed the basis for ^{1}H,^{13}C,^{15}N backbone resonance assignment using Targeted Acquisition (32, 34), followed by manual inspection. In the dark spectra, 75% of all assignable residues were assigned for the dark-adapted state (Fig. 2). In the light spectra we assigned 73% of all assignable residues (Fig. 2). Many assignments were transferred from the dark-adapted to the light state spectra based on identical chemical shifts. Using our illumination conditions (660 nm), the light state is estimated to have an occupancy of 65% (13). Accordingly, our NMR spectra showed residual intensities of dark-adapted peaks in the “light” 2D spectra (Fig. S1A in the Supporting Material). However, in “light” 3D spectra, the intensities were below detection limit for many of the dark-adapted signals. Therefore, the assignment of light state signals was unambiguous for the majority of the peaks. In

both states, unassigned residues cluster in the core region and the helical spine of the protein, likely due to poor proton back-exchange. Attempts to favor exchange was performed by switching the protein between dark and light state multiple times and at elevated temperatures, without any success.

Light state contribution detected for the dark-adapted protein

Interestingly, the NMR data indicate that the dark-adapted proteins contain a contribution from the light state (Fig. S1B in the Supporting Material). Peaks assigned for the light state were present in the "dark" spectra, and the intensities increased over time in darkness. Integration of multiple light state peaks in the dark detected [$^{1}H^{15}N$]-TROSY spectrum showed that the light state peaks reached an intensity maximum of 10-15% of the equivalent dark-adapted state peak. This is corroborated by UV-Vis spectra which show an increase of far-red absorption when left in dark, corresponding to also 10-15% light (Fig. S1, C and D in the Supporting Material). Our data thereby demonstrate directly that a light state conformation exist even when *Dr*BphP is illuminated with far-red light and left in the dark.

Structural heterogeneity in the PHY-tongue region

Next, we turned our attention to the PHY tongue region. We could fully assign the tongue arms (residues 444-449 and 465-476) in the light state, including several highly conserved residues, but the tongue could not be resolved in the dark-adapted state (Fig. 2). We attribute the absence of tongue peaks in the dark-adapted state to peak broadening due to structural heterogeneity on a micro- to millisecond time scale. This conclusion is rationalized by considering that the chemical shift of a nucleus can be altered when there is a conformational change in the protein. If the exchange between two conformations is slow, the different states of the nucleus will appear as two narrow peaks in the NMR spectrum. For fast exchange, the peaks sharpen into a single peak at the averaged position. When the rate of interconversion is at an intermediate level, the peaks merge into one broad low amplitude peak, beyond detection, at the population averaged position. This occurs on the time scale of micro- to milliseconds. The absence of

tongue peaks in the dark state are thus an indication of structural heterogeneity with micro-to milliseconds exchange kinetics.

To strengthen this conclusion, we labeled all lysines in the protein with ^{13}C and ^{15}N (Fig. 3A). K476 in *Dr*BphP$_{mon}$ is located in the upper part of the tongue. One of the light state peaks for the lysine-labeled sample (Fig. 3B) disappeared upon mutation of K476 into alanine (circled), which identified the position of the K476 resonance in the spectrum (Fig. 3C). The same lysine signal also disappeared when photoconverting the sample into the dark-adapted state. This strongly supports our interpretation that conformational heterogeneity exists in the PHY-tongue in dark-adapted state.

To exclude rapid exchange with the bulk-water as the cause for the loss of NMR signals in the PHY tongue in dark-adapted state, we performed a number of test experiments. Factors that affect the rate of this exchange are hydrogen bonding, temperature and pH. We therefore recorded NMR data for the lysine-labelled sample in the temperature range of 15-55°C, but were not able to retrieve the lysine signal for the dark-adapted state (Fig S2 in the Supporting Material). Furthermore, K476 is also modeled as hydrogen bonded to the other β-strand in crystal structures, which should slow down the exchange with bulk water. Also [$^{1}H^{15}N$]-TROSYs were recorded at pH 6.9, 6.0 and 4.8, as lowering the pH should slow down the rate of bulk-water exchange. None of the tested pH could retrieve the K476 lysine signal in the tongue region (Figure S3 in the Supporting Material). This excludes the alternative explanation, strengthening our conclusion that structural heterogeneity of the PHY tongue is present.

The other solvent-exposed lysine (K460) was also assigned using a K460A mutant (Fig S4 in the Supporting Material). In the light state, this lysine appears as two separate peaks (arrows in Fig. 3B). This is due to the presence of two separate states, which can be in slow exchange, while in the dark state only one of the peaks appear. This indicates that K460 and K476 do not belong to the same structural element and that they have different structural dynamics. More experiments are needed to confirm this and to investigate the dynamic properties of the lysine (at 8.6 ppm) that shows as a peak doubling in the dark state in the K476A mutant. A K177A mutant was also created, which precipitated most likely due to a destabilizing effect of the mutation.

Secondary chemical shift analysis of the PHY-tongue in light state

Variations in chemical shifts from random coil values (33), so-called secondary chemical shifts, provide insights into secondary structure propensities. Positive values of Cα, CO and negative values of Cβ indicate α-helical structure, and the opposite indicate β-strand structure (35). A comparison of the secondary chemical shift calculated with TALOS-N using assigned chemical shifts(36) to the crystal structure (Figure S5 in the Supporting Material) show an overall good agreement. In the light state (Fig. 4A), the secondary chemical shifts for the tongue region strongly indicate α-helical structure for the second arm (residue 465-476), but also the presence of β-strand structure in the first arm (residue 444-449). Prediction of the secondary structures using the CSI (chemical shift index) 3.0 web server (37) confirm this interpretation (see Fig. 4B). Two stable secondary structure elements for the tongue region in the light state are detected, which is in contrast to the conformationally heterogeneous dark state.

Discussion

For a long time it was believed that the specific function of a protein is predetermined by its unique three-dimensional structure. Proteins are, however, not solid rigid bodies and the role of dynamics in the molecular mechanisms of these macromolecules have become increasingly clear.

We propose that the modulation of structural heterogeneity of the tongue region of *Dr*BphP$_{mon}$ is of functional relevance (Fig. 5). Structural heterogeneity in phytochromes has been reported for residues surrounding the chromophore in smaller constructs, which excluded the PHY domain (18, 23, 24, 38). The β-strand structure of the PHY tongue in the dark state, as detected by crystallography, should be considered as one of the conformations present in solution that is selected from a two or more structures that preferentially crystallizes. This conformational heterogeneity in the dark-adapted state can explain why *Dr*BphP can adopt light state-like crystals in darkness (39).

As such, the signaling mechanism does not simply involve a change of fold in the PHY tongue, as previously described (13, 26–28), but instead we suggest that the activity in *Dr*BphP is triggered by altering the equilibrium between the structural heterogenous dark state towards the ordered state in light. We suggest that the decreased conformational flexibility in the light state ”locks” the phytochrome, altering the activity of the protein. This modulation of heterogeneity could be transferred to the helical spine, and thereby further to the output domains (40).

We have performed a solution NMR analysis of the large system of *Dr*BphP$_{mon}$, gaining insight of the important signaling tongue region using a laser-triggered approach, exciting the protein inside the NMR magnet in a non-continuous way during acquisition. Our study demonstrates that it is critical to study phytochromes in solution to reveal both the structure and the dynamic behavior of the protein in different functional states. The reported backbone chemical shift assignment is the basis for further NMR investigations, and with the first partial assignment of a complete photosensory module of *Dr*BphP$_{mon}$, we have opened up for studying the protein with atomic precision in solution, giving important information about the dynamic personalities of the phytochrome.

Conclusion

We conclude that the PHY-tongue region undergoes a transition from a structural heterogenous state to an ordered state upon light-activation. Since the dynamics of the PHY tongue are directly controlled by the light conditions, we suggest that the alteration of the structure equilibrium towards the ordered light state is of biological significance for the photomodulation of phytochromes.

Author contributions

E. Gustavsson and L. Isaksson planned the project together with S. Westenhoff., C. Persson., V. Orekhov., B. G. Karlsson., U. Brath. and J.A. Ihalainen.. E. Gustavsson., L. Isaksson., and L.Vrhovac produced and purified all samples and performed all measurements and analysis together with V. Orekhov., M. Mayzel. and C. Persson.. E. Gustavsson., C. Persson., and L. Isaksson. performed the backbone assignment. E. Gustavsson., L. Isaksson., and S. Westenhoff. wrote the manuscript with edits by J.A. Ihalainen.

Acknowledgements

We would like to thank Sami Mäkelä, Marjo Haapakoski, and Ilkka Minkkinen for initial temperature stability experiments performed with UV/Vis spectrophotometry. We also thank Michal Maj and Magnus Wolf-Watz for feedback for the manuscript. Sebastian Westenhoff thanks the Knut and Alice Wallenberg Foundation for an Academy Fellowship. Janne Ihalainen acknowledges the Academy of Finland grant 296135 and Jane and Aatos Erkko foundation. Vladislav Orekhov thanks the support by the Swedish Research Council (Research Grant 201504614). NMR spectroscopy was carried out at the Swedish NMR Centre at University of Gothenburg, supported by the Knut and Alice Wallenberg Foundation (NMR for Life) and the Science for Life Laboratory (SciLifeLab).

The authors declare that they do not have any conflicts of interest.

References

1. Gan, F., S. Zhang, N.C. Rockwell, S.S. Martin, J.C. Lagarias, and D.A. Bryant. 2014. Extensive remodeling of a cyanobacterial photosynthetic apparatus in far-red light. Science (80-.). 345: 1312–1317.
2. Legris, M., C. Klose, E.S. Burgie, C.C.R. Rojas, M. Neme, A. Hiltbrunner, P.A. Wigge, E. Schäfer, R.D. Vierstra, and J.J. Casal. 2016. Phytochrome B integrates light and temperature signals in Arabidopsis. Science (80-.). 354: 897–900.
3. Quail, P.H. 2002. Phytochrome photosensory signalling networks. Nat. Rev. Mol. Cell Biol. 3: 85–93.
4. Yeh, K. 1997. A Cyanobacterial Phytochrome Two-Component Light Sensory System. Science (80-.). 277: 1505–1508.
5. Hughes, J., T. Lamparter, F. Mittmann, E. Hartmann, W. Gärtner, A. Wilde, and T. Börner. 1997. A prokaryotic phytochrome. Nature. 386: 663–663.
6. Davis, S.J. 1999. Bacteriophytochromes: Phytochrome-Like Photoreceptors from Nonphotosynthetic Eubacteria. Science (80-.). 286: 2517–2520.
7. Fankhauser, C. 2001. The Phytochromes, a Family of Red/Far-red Absorbing Photoreceptors. J. Biol. Chem. 276: 11453–11456.
8. Rockwell, N.C., D. Duanmu, S.S. Martin, C. Bachy, D.C. Price, D. Bhattacharya, A.Z. Worden, and J.C. Lagarias. 2014. Eukaryotic algal phytochromes span the visible spectrum. Proc. Natl. Acad. Sci. 111: 3871–3876.
9. Kim, C.K., A. Adhikari, and K. Deisseroth. 2017. Integration of optogenetics with complementary methodologies in systems neuroscience. Nat. Rev. Neurosci. .
10. Auldridge, M.E., K.A. Satyshur, D.M. Anstrom, and K.T. Forest. 2012. Structure-guided Engineering Enhances a Phytochrome-based Infrared Fluorescent Protein. J. Biol. Chem. 287: 7000–7009.
11. Rockwell, N.C., Y.-S. Su, and J.C. Lagarias. 2006. Phytochrome structure and signaling mechanisms. Annu. Rev. Plant Biol. 57: 837–858.
12. Edlund, P., H. Takala, E. Claesson, L. Henry, R. Dods, H. Lehtivuori, M. Panman, K. Pande, T. White, T. Nakane, O. Berntsson, E. Gustavsson, P. Båth, V. Modi, S. Roy-Chowdhury, J. Zook, P. Berntsen, S. Pandey, I. Poudyal, J. Tenboer, C. Kupitz, A. Barty, P. Fromme, J.D. Koralek, T. Tanaka, J. Spence, M. Liang, M.S. Hunter, S. Boutet, E. Nango, K. Moffat, G. Groenhof, J. Ihalainen, E.A. Stojković, M. Schmidt, and S. Westenhoff. 2016. The room temperature crystal structure of a bacterial phytochrome determined by serial femtosecond crystallography. Sci. Rep. 6: 35279.
13. Takala, H., A. Björling, O. Berntsson, H. Lehtivuori, S. Niebling, M. Hoernke, I. Kosheleva, R. Henning, A. Menzel, J.A. Ihalainen, and S. Westenhoff. 2014. Signal amplification and transduction in phytochrome photosensors. Nature. 509: 245–248.
14. Essen, L.-O., J. Mailliet, and J. Hughes. 2008. The structure of a complete phytochrome sensory module in the Pr ground state. Proc. Natl. Acad. Sci. 105: 14709–14714.
15. Yang, X., J. Kuk, and K. Moffat. 2008. Crystal structure of Pseudomonas aeruginosa bacteriophytochrome: photoconversion and signal transduction. Proc. Natl. Acad. Sci. U. S. A. 105: 14715–14720.
16. van der Lee, R., M. Buljan, B. Lang, R.J. Weatheritt, G.W. Daughdrill, A.K. Dunker, M. Fuxreiter, J. Gough, J. Gsponer, D.T. Jones, P.M. Kim, R.W. Kriwacki, C.J. Oldfield, R. V. Pappu, P. Tompa, V.N. Uversky, P.E. Wright, and M.M. Babu. 2014. Classification of Intrinsically Disordered Regions and Proteins. Chem. Rev. .
17. Frueh, D.P., A.C. Goodrich, S.H. Mishra, and S.R. Nichols. 2013. NMR methods for structural studies of large monomeric and multimeric proteins. Curr. Opin. Struct. Biol. 23: 734–739.
18. Lim, S., Q. Yu, S.M. Gottlieb, C.-W. Chang, N.C. Rockwell, S.S. Martin, D. Madsen, J.C. Lagarias, D.S. Larsen, and J.B. Ames. 2018. Correlating structural and photochemical

heterogeneity in cyanobacteriochrome NpR6012g4. Proc. Natl. Acad. Sci. 115: 4387–4392.
19. Cornilescu, C.C., G. Cornilescu, E.S. Burgie, J.L. Markley, A.T. Ulijasz, and R.D. Vierstra. 2014. Dynamic Structural Changes Underpin Photoconversion of a Blue/Green Cyanobacteriochrome between Its Dark and Photoactivated States. J. Biol. Chem. 289: 3055–3065.
20. Strauss, H.M., J. Hughes, and P. Schmieder. 2005. Heteronuclear Solution-State NMR Studies of the Chromophore in Cyanobacterial Phytochrome Cph1 †. Biochemistry. 44: 8244–8250.
21. Rudiger, W., F. Thummler, E. Cmiel, and S. Schneider. 1983. Chromophore structure of the physiologically active form (Pfr) of phytochrome. Proc. Natl. Acad. Sci. 80: 6244–6248.
22. Lagarias, J.C., and H. Rapoport. 1980. Chromopeptides from phytochrome. The structure and linkage of the PR form of the phytochrome chromophore. J. Am. Chem. Soc. 102: 4821–4828.
23. Song, C., G. Psakis, C. Lang, J. Mailliet, W. Gartner, J. Hughes, and J. Matysik. 2011. Two ground state isoforms and a chromophore D-ring photoflip triggering extensive intramolecular changes in a canonical phytochrome. Proc. Natl. Acad. Sci. 108: 3842–3847.
24. Kim, P.W., N.C. Rockwell, S.S. Martin, J.C. Lagarias, and D.S. Larsen. 2014. Dynamic Inhomogeneity in the Photodynamics of Cyanobacterial Phytochrome Cph1. Biochemistry. 53: 2818–2826.
25. Velazquez Escobar, F., D. von Stetten, M. Günther-Lütkens, A. Keidel, N. Michael, T. Lamparter, L.-O. Essen, J. Hughes, W. Gärtner, Y. Yang, K. Heyne, M.A. Mroginski, and P. Hildebrandt. 2015. Conformational heterogeneity of the Pfr chromophore in plant and cyanobacterial phytochromes. Front. Mol. Biosci. 2: 37.
26. Yang, X., Z. Ren, J. Kuk, and K. Moffat. 2011. Temperature-scan cryocrystallography reveals reaction intermediates in bacteriophytochrome. Nature. .
27. Ihalainen, J.A., E. Gustavsson, L. Schroeder, S. Donnini, H. Lehtivuori, L. Isaksson, C. Thöing, V. Modi, O. Berntsson, B. Stucki-Buchli, A. Liukkonen, H. Häkkänen, E. Kalenius, S. Westenhoff, and T. Kottke. 2018. Chromophore-Protein Interplay during the Phytochrome Photocycle Revealed by Step-Scan FTIR Spectroscopy. J. Am. Chem. Soc. .
28. Burgie, E.S., J. Zhang, and R.D. Vierstra. 2016. Crystal Structure of Deinococcus Phytochrome in the Photoactivated State Reveals a Cascade of Structural Rearrangements during Photoconversion. Structure. 24: 448–457.
29. Takala, H., S. Niebling, O. Berntsson, A. Björling, H. Lehtivuori, H. Häkkänen, M. Panman, E. Gustavsson, M. Hoernke, G. Newby, F. Zontone, M. Wulff, A. Menzel, J.A. Ihalainen, and S. Westenhoff. 2016. Light-induced structural changes in a monomeric bacteriophytochrome. Struct. Dyn. 3: 054701.
30. Buchli, B., S.A. Waldauer, R. Walser, M.L. Donten, R. Pfister, N. Blochliger, S. Steiner, A. Caflisch, O. Zerbe, and P. Hamm. 2013. Kinetic response of a photoperturbed allosteric protein. Proc. Natl. Acad. Sci. 110: 11725–11730.
31. Vranken, W.F., W. Boucher, T.J. Stevens, R.H. Fogh, A. Pajon, M. Llinas, E.L. Ulrich, J.L. Markley, J. Ionides, and E.D. Laue. 2005. The CCPN data model for NMR spectroscopy: Development of a software pipeline. Proteins Struct. Funct. Bioinforma. 59: 687–696.
32. Isaksson, L., M. Mayzel, M. Saline, A. Pedersen, J. Rosenlöw, B. Brutscher, B.G. Karlsson, and V.Y. Orekhov. 2013. Highly Efficient NMR Assignment of Intrinsically Disordered Proteins: Application to B- and T Cell Receptor Domains. PLoS One. 8: e62947.
33. Wishart, D., and B. Sykes. 1994. The 13C Chemical-Shift Index: A simple method for the identification of protein secondary structure using 13C chemical-shift data. J. Biomol. NMR. 4: 171–180.
34. Jaravine, V.A., A. V Zhuravleva, P. Permi, I. Ibraghimov, and V.Y. Orekhov. 2008. Hyperdimensional NMR Spectroscopy with Nonlinear Sampling. J. Am. Chem. Soc. 130: 3927–3936.
35. Dyson, H.J., and P.E. Wright. 2004. Unfolded Proteins and Protein Folding Studied by NMR. Chem. Rev. 104: 3607–3622.
36. Shen, Y., and A. Bax. 2013. Protein backbone and sidechain torsion angles predicted from NMR

chemical shifts using artificial neural networks. J. Biomol. NMR. 56: 227–241.
37. Hafsa, N.E., D. Arndt, and D.S. Wishart. 2015. CSI 3.0: a web server for identifying secondary and super-secondary structure in proteins using NMR chemical shifts. Nucleic Acids Res. 43: W370–W377.
38. Rockwell, N.C., S.S. Martin, A.G. Gulevich, and J.C. Lagarias. 2014. Conserved Phenylalanine Residues Are Required for Blue-Shifting of Cyanobacteriochrome Photoproducts. Biochemistry. 53: 3118–3130.
39. Takala, H., H.K. Lehtivuori, O. Berntsson, A. Hughes, R. Nanekar, S. Niebling, M. Panman, L. Henry, A. Menzel, S. Westenhoff, and J.A. Ihalainen. 2018. On the (un)coupling of the chromophore, tongue interactions, and overall conformation in a bacterial phytochrome. J. Biol. Chem. 293: 8161–8172.
40. Gourinchas, G., U. Heintz, and A. Winkler. 2018. Asymmetric activation mechanism of a homodimeric red light-regulated photoreceptor. Elife. 7: e34815.

Figure legends

Figure 1. 2D [$^{1}H^{15}N$]-TROSYs for the dark and light state. (A) 2D [$^{1}H^{15}N$]-TROSY of the dark-adapted state. The assignments are annotated with one-letter amino acid code and the sequence number. The crowded mid-region is shown as an insert. BMRB Entry 27783**.** (B) Annotated 2D [$^{1}H^{15}N$]- TROSY of the light state. The crowded mid-region is shown as an insert. BMRB Entry 27784.

Figure 2. Backbone chemical shift assignment of the dark (left) and light (right) state of the PAS-GAF-PHY photosensory module. Assigned residues (green) were mapped on structures with PDB codes: 4Q0J and 4O01, respectively. The biliverdin chromophore is colored in orange and the helical spine is marked in the light state. The PHY-tongue and its refolding between the dark and the light state is highlighted with a ring.

Figure 3. Lysine labeling of *Dr*BphP$_{mon.}$ (A) Structure with lysines marked in red (PDB ID: 4Q0J). (B) [$^{1}H^{15}N$]-TROSY of lysines, where the tongue lysine disappears in the dark state due to structural dynamics on micro- to millisecond timescale. K460 that demonstrates two different conformations in light and one conformation in dark is marked with arrows. (C) [$^{1}H^{15}N$]-TROSY of K476A mutant identifies the lysine located in the tongue, circled in red in both B and C.

Figure 4. Secondary structure elements in the light state for the two tongue arms in *Dr*BphP$_{mon.}$ (A) Calculated secondary chemical shifts in light form, which corresponds well with a β-strand structure in the first arm of the tongue, while the second arm is of an α-helical nature. Conserved residues are marked with an asterix. (B) The predicted secondary structure probability from H, NH, Cα, Cβ and CO chemical shifts calculated by CSI 3.0 (37).

Figure 5. Transition from the **structurally heterogeneous** dark state to the **ordered** light state. Conformational fluctuation of the chromophore binding pocket has previously been described for the dark state around the chromophore (18, 23). Our data reveal that this structural heterogeneity extends far into the PHY-tongue in *Dr*BphP. Further we could show that the tongue adopts an ordered α-helix and β-strand structure in light state. We suggest that this transition locks the *Dr*BphP in its photoactivated state. PDB codes: 4O0P (dark-adapted state) and 5C5K (light state).

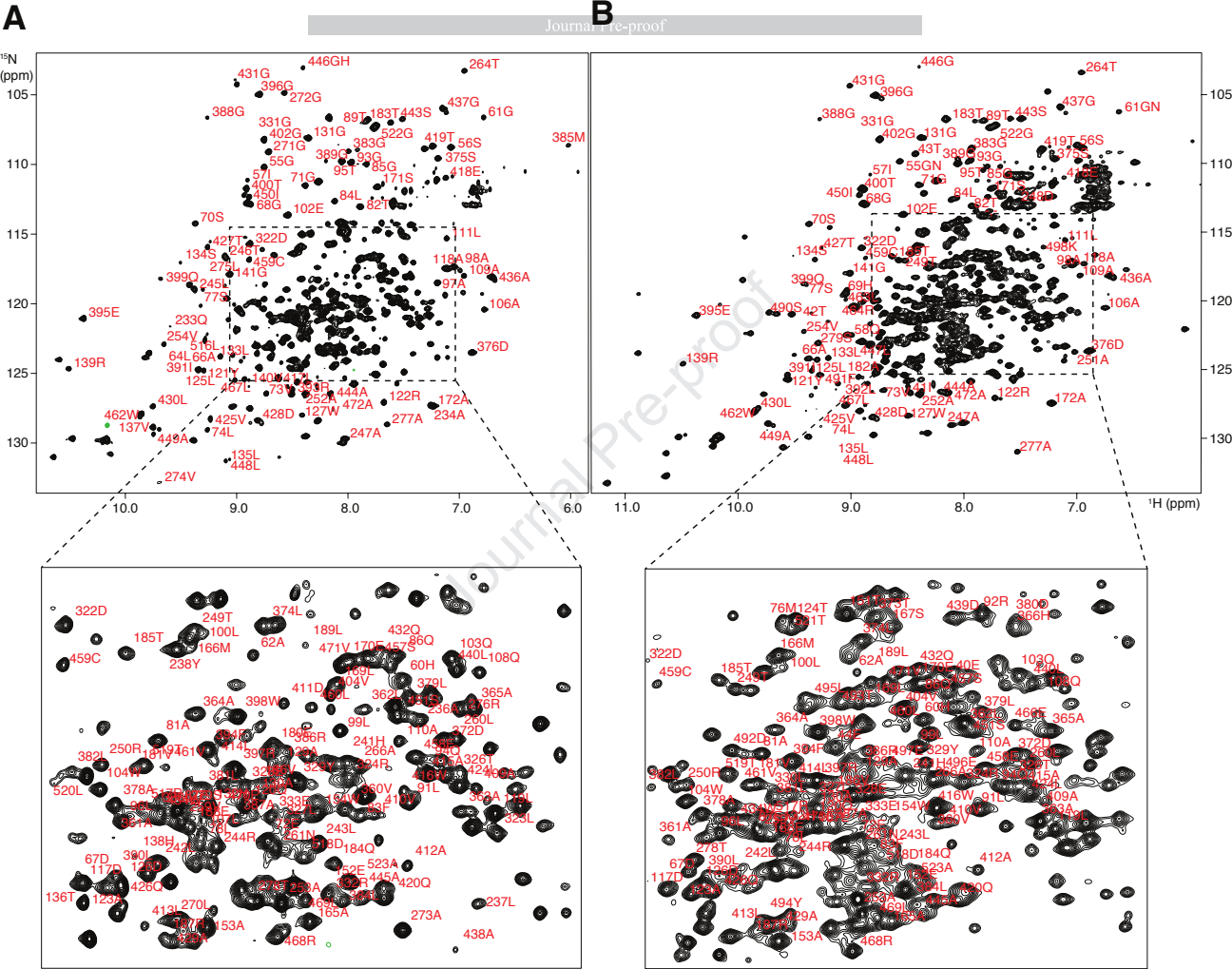

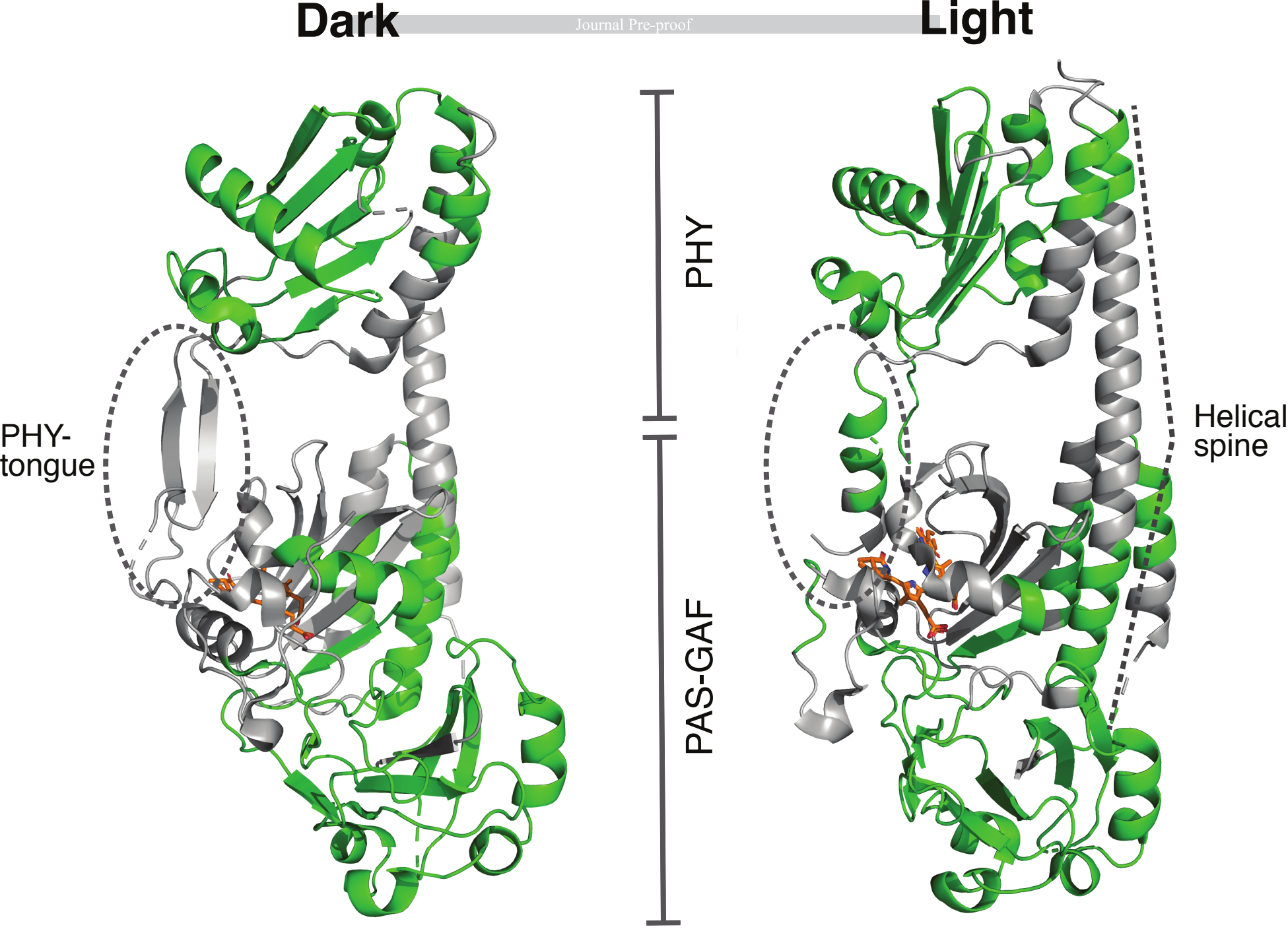

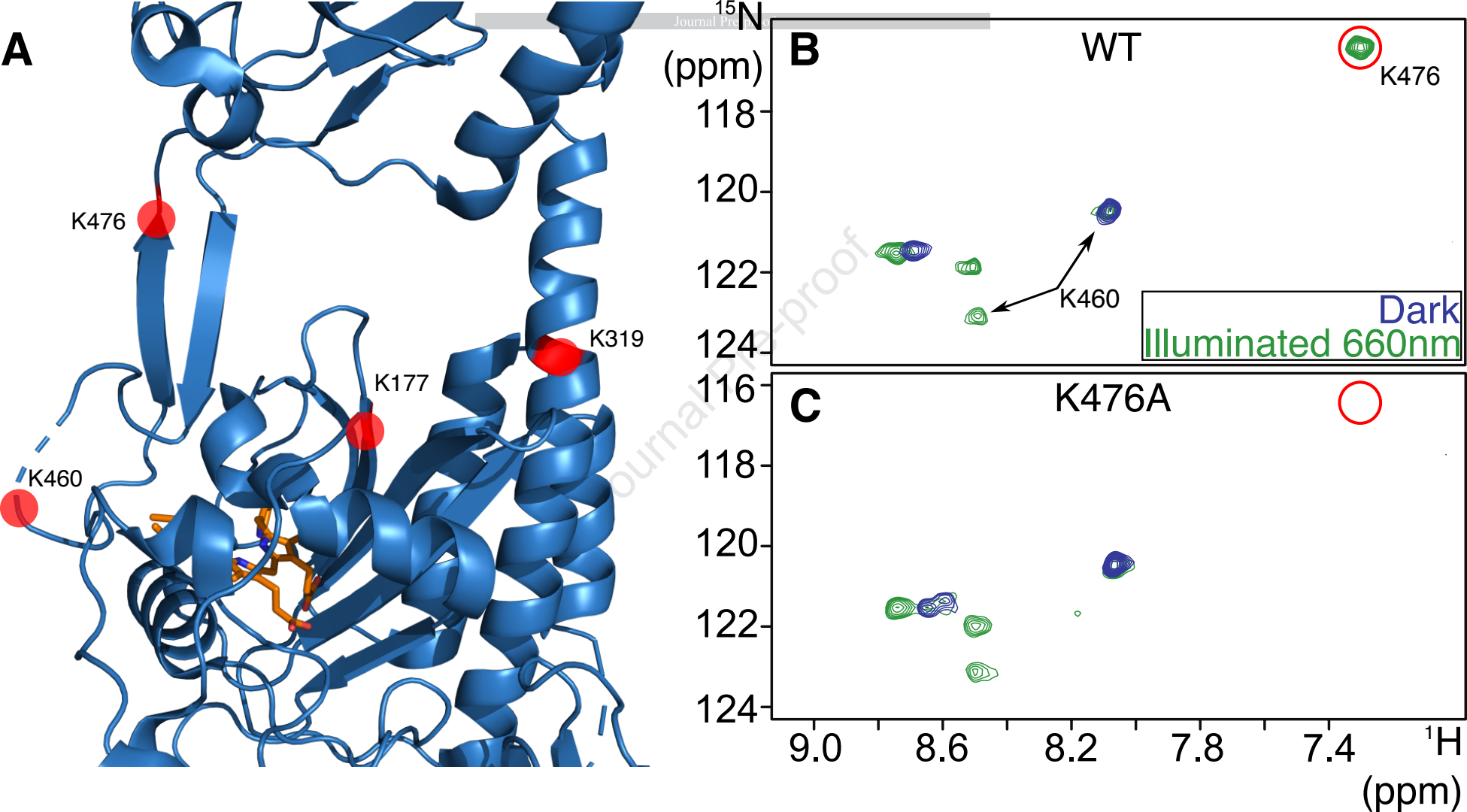
A
K476
K319
K177
K460
B
WT
K476
K460
Dark
Illuminated 660nm
C
K476A
^{15}N (ppm)
118
120
122
124
116
118
120
122
124
9.0
8.6
8.2
7.8
7.4
^{1}H (ppm)

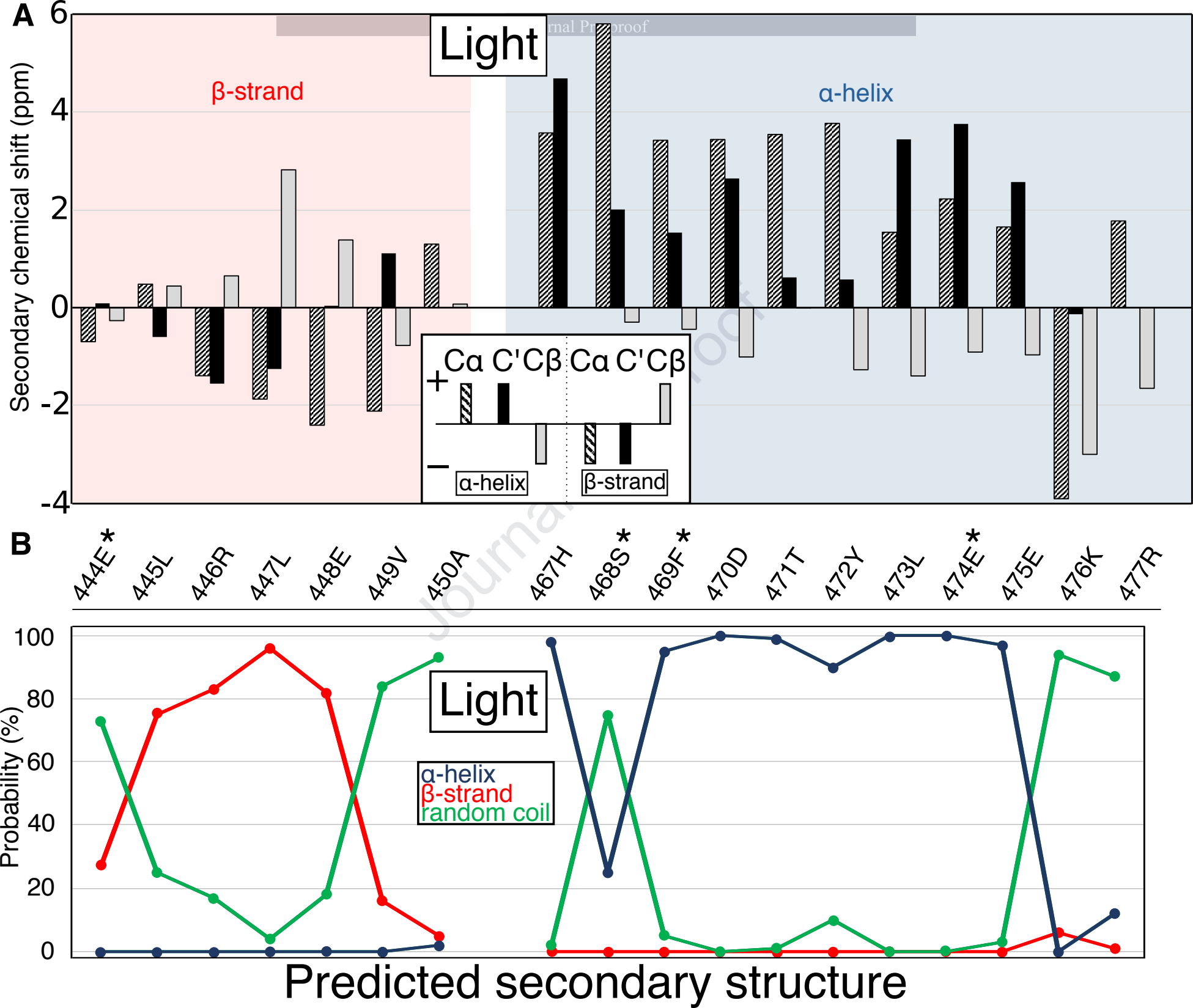
A
Light
β-strand
α-helix
Secondary chemical shift (ppm)
6
4
2
0
-2
-4
Cα C'Cβ Cα C'Cβ
+
−
α-helix
β-strand
B
444E*
445L
446R
447L
448E
449V
450A
467H
468S*
469F*
470D
471T
472Y
473L
474E*
475E
476K
477R
Light
α-helix
β-strand
random coil
Probability (%)
100
80
60
40
20
0
Predicted secondary structure